Progress In Electromagnetics Research M, Vol. 31, 103–116, 2013

DESIGN OF A LOW SIDELOBE 4D PLANAR ARRAY INCLUDING MUTUAL COUPLING

Quanjiang Zhu, Shiwen Yang*, Ruilin Yao, and Zaiping Nie

School of Electronic Engineering, University of Electronic Science and Technology of China (UESTC), Chengdu 611731, China

Abstract—An efficient approach is presented for the design of a low sidelobe four-dimensional (4D) planar antenna array, taking into account mutual coupling and platform effect. The approach is based on the combination of the active element patterns and the differential evolution (DE) algorithm. Different from linear and circular arrays, the mutual coupling compensation in a planar array is more complicated since it requires numerous data of the active element patterns in different azimuth planes. In order to solve this problem, a useful interface program is developed to get these data from commercial software HFSS automatically. Also different from conventional low sidelobe arrays with tapered amplitude excitations, the low sidelobe in the 4D array is realized using time-modulation technique under uniform static amplitude and phase conditions. The DE algorithm is used to optimize the time sequences which are equivalent to the complex excitations in conventional arrays. Both computed results and simulated results in HFSS show that a -30 dB sidelobe pattern can be synthesized in a 76-element planar array with an octagonal ground plane and a radome, thus verifying the proposed approach.

1. INTRODUCTION

Four-dimensional (4D) antenna arrays, which are also termed as time modulated arrays in literature [1–8], are formed by introducing a fourth dimension, time, into conventional antenna arrays operating in the 3-dimensional space. As compared to conventional arrays, the 4D arrays have much more flexibility in pattern synthesis, due to the additional degree of design freedom, time. For example, low sidelobe level (SLL) patterns can be synthesized in 4D arrays

Received 22 February 2013, Accepted 27 May 2013, Scheduled 30 May 2013

* Corresponding author: Shiwen Yang (swnyang@uestc.edu.cn).

with uniform static amplitude and phase excitations. In the past decade, many studies have been carried out to synthesize desired patterns and suppress the sideband level (SBL) in 4D linear and planar arrays using various optimization algorithms [3–11]. Recently, some studies show that 4D arrays have promising potentials for some practical applications, such as harmonic beamforming without phase shifting [12, 13], direction finding [14, 15], monopulse radar design [16, 17], adaptive nulling [18, 19], and directional modulation for secure communication [20]. All these distinct advantages in 4D arrays are based on the exploitation and utilization of the sideband signals caused by time modulation.

This paper focuses on the pattern synthesis of 4D planar arrays, taking into account the mutual coupling and platform effect. Although the pattern synthesis of 4D planar arrays has been reported in [9–11] where isotropic elements are used, the mutual coupling effect has not been addressed. Mutual coupling among antenna elements in antenna arrays can strongly affect the radiation pattern, especially in small- and medium-sized arrays [21]. Many efforts have been made to compensate for the mutual coupling effect through the coupling impendence matrix combining numerical computation technique (e.g., method of moments) [22–24]. They are very efficient descriptions of the coupling effect for linear and circular arrays with simple elements. However, the approach is no longer adequate for a planar array with tens of complex elements and a platform, as the computation of the coupling matrix is a very heavy burden.

The active element pattern method is a very simple but powerful tool to account for the mutual coupling and platform effect [25–29]. The active element pattern of an array is defined as the radiation pattern of the array when a single radiating element is driven and all the other elements are terminated with matched loads. The active element patterns have a specific relationship with mutual impedance matrices in array antennas. The later can be determined from the former [30, 31]. The radiation pattern of a fully excited array can be expressed as the sum of the active element patterns scaled corresponding complex excitations, without taking into account the array factor. Since the active element patterns are produced in the presence of the mutual coupling and platform effects, the array response includes mutual coupling and platform effects. The active element pattern can be obtained by either measurement or full-wave simulation of the array. Of course, the latter is more preferable for most antenna engineers nowadays, as this task can be fulfilled easily by several commercial simulation solvers, such as HFSS and CST. After the data of active element patterns are obtained and stored, the pattern

synthesis can be performed using global optimization algorithms (e.g., differential evolution [3, 32–34]).

The paper is organized as follows. In Section 2, a 76-element printed dipole planar array is presented. Simulated results show that the array elements can operate from 2.0 GHz to 4.0 GHz, with an active VSWR of less than 1.5. In Section 3, some mathematical formulations of 4D arrays are presented, and field computation disciplines in different coordinate systems are explained. Then an effective procedure is introduced to automatically acquire the data of active element patterns of individual elements in different azimuth planes. Combining the stored active element pattern data, the DE algorithm is used to optimize the time sequences for synthesizing a low sidelobe pattern. In Section 5, some numerical results are reported to demonstrate the effectiveness of the proposed pattern synthesis approach, including computed patterns and simulated patterns by HFSS. Finally, some conclusions are drawn.

2. DESIGN OF THE PLANAR ARRAY

The main difference between 4D arrays and conventional arrays lies in the feeding network. Different from conventional low SLL array with tapered amplitude excitations, the 4D planar array presented in this paper is time-modulated to achieve equivalent amplitude weighting at the center frequency and both amplitude and phase weighting at the sideband frequencies. In this paper, commercial software HFSS is used to design and simulate the 4D planar arrays [35].

Figure 1 shows a 4D planar array consisting of 76 printed dipoles.

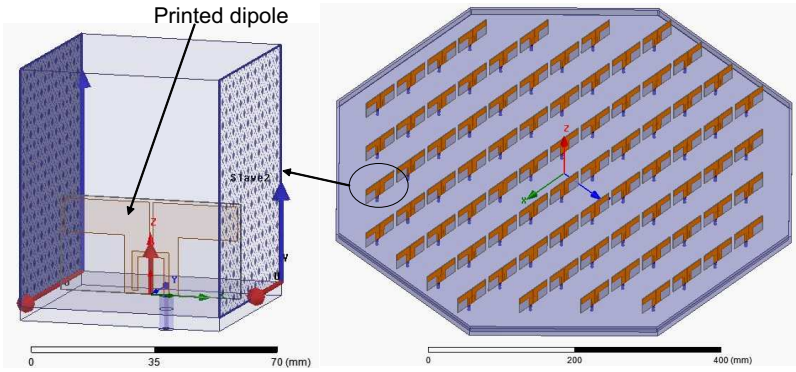

Figure 1. Geometry of the 76-element planar array with an octagonal ground plane.

For simplicity, the feeding network including the RF switches is not simulated in HFSS, since it does not affect of the radiation pattern of the 4D array. The elements are uniformly laid out in a rectangular lattice in the XY plane, with an inter-element separation of half wavelength at 2.5 GHz. The planar array is covered by a radome and backed on an octagonal ground plane.

Figure 2 illustrates the simulated active VSWR of an antenna element in an infinite array where master and slave boundaries are used. Figure 3 shows the simulated active VSWRs of different elements in the 76-element array (the No. of antenna elements is referred to Figure 6). As can be seen, the array elements can be used to operate from 2.0 GHz to 4.0 GHz (VSWR < 1.5). The VSWRs of the elements near the center of the array (e.g., No. 1, 2 and 6) are almost the same as that of a single element in an infinite array. This is due to that mutual coupling effect is most significant between neighboring elements, and the center elements experience approximately the same electromagnetic environment as an element in an infinite array. The active VSWRs of the elements near the edges of the array (e.g., No. 4 and 5) deteriorate, since they experience a different electromagnetic coupling environment as the elements near the center. The good impendence matching performance is necessary to ensure that the array has a higher realized gain, whose definition includes the effect of reflected power [25].

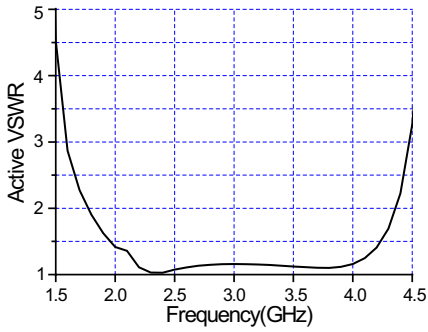

Figure 2. The active VSWR of an element in an infinite array.

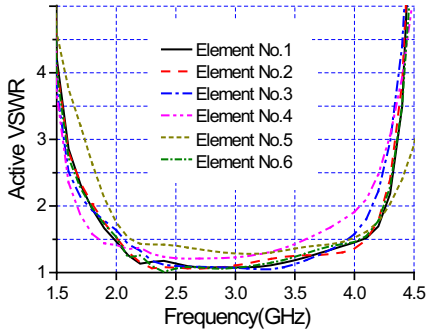

Figure 3. The active VSWRs of different elements in the 76-element planar array when all elements are uniformly excited.

As the geometry of the 76-element array is almost symmetrical with respect to the XZ and YZ planes, both the two planes are set as symmetry boundaries. The 76-element array is reduced into a 19-element subarray, as shown in Figure 4. Assigning symmetry

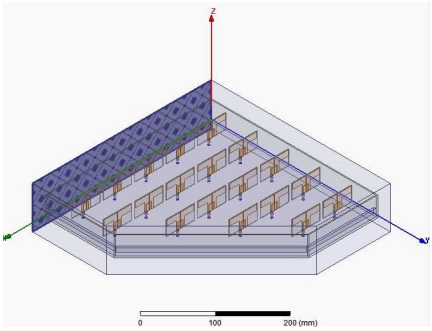

Figure 4. Geometry of the 19-element subarray obtained by splitting the 76-element array from the XZ and YZ plane.

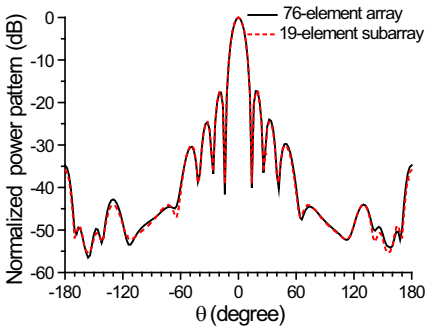

Figure 5. Comparison of the radiation patterns of the 76-element array and the 19-element subarray in $\varphi = 10^\circ$ plane.

boundaries will reduce the computation burden significantly for the pattern synthesis in the following parts. To validate the model, the radiation patterns of the full array shown in Figure 1 and the subarray shown in Figure 4 are compared. Figure 5 illustrates the comparison of the radiation patterns of the 76-element array and the 19-element subarray in $\varphi = 10^\circ$ plane. The pattern of the subarray with symmetry boundaries matches well with the pattern of the full array.

3. PATTERN SYNTHESIS APPROACH

3.1. Mathematical Formulation of 4D Arrays

In this paper, the 4D planar array is supposed to operate at the center frequency $f_0 = 2.5\,\text{GHz}$, with uniform static amplitude and phase excitations. In order to synthesize a low SLL pattern, the array is time-modulated by RF switches and its time sequences will be optimized in the subsequent part. The time modulation period is set as T_p, with a time modulation frequency $f_p = 1/T_p$ ($f_p \ll f_0$, the radiation pattern is independent of f_p). For simplicity, the time modulation scheme of pulse shifting proposed by Poli and Rocca is adopted [36], which is an appropriate trade-off between the flexibility and complexity of the time sequences. The periodic switch on-off time function $U_i(t)$ for the ith element can be given by

$$U_i(t) = \begin{cases} 1 & t_i \le t \le t_i + \tau_i \\ 0 & \text{others} \end{cases} \tag{1}$$

where $0 \le t_i \le 1$ and $0 \le \tau_i \le 1$. t_i and τ_i denote the switch-on time and on-off time interval for the ith element, respectively. Both of them

are normalized values.

The time modulation in 4D arrays can bring on equivalent amplitude excitations at the center frequency, and both amplitude and phase excitations at the sideband frequencies in a time-average sense. Using Fourier series decomposition approach [2], the equivalent complex excitations for the ith element at the center frequency f_0 and the first order sideband frequency $f_0 + f_p$ are expressed as

$$\begin{aligned} \mathbf{w}^0(i) &= \tau_i \\ \mathbf{w}^1(i) &= \tau_i \sin \mathrm{c}(\pi\tau_i) \cdot e^{-j\pi(2t_i+\tau_i)} \end{aligned} \tag{2}$$

where $\boldsymbol{w}^0(i)$ and $\boldsymbol{w}^1(i)$ denote the complex excitations at f_0 and f_0+f_p, respectively. Since the higher order sideband levels of 4D antenna arrays with pulse shifting are usually much lower than that of the first sideband, only the equivalent complex excitations at the center frequency and the first sideband are considered in this paper.

3.2. Coordinate System in HFSS

By the principle of superposition, the radiation vector field of the fully excited array can be expressed as the superposition of the active element patterns scaled by corresponding complex excitations, given by

$$\begin{aligned} \mathbf{E}_\theta^m(\theta,\varphi) &= \sum_{i=1}^{N} \mathbf{w}^m(i) \cdot \mathbf{E}_\theta(i,\theta,\varphi), \\ \mathbf{E}_\varphi^m(\theta,\varphi) &= \sum_{i=1}^{N} \mathbf{w}^m(i) \cdot \mathbf{E}_\varphi(i,\theta,\varphi) \end{aligned} \tag{3}$$

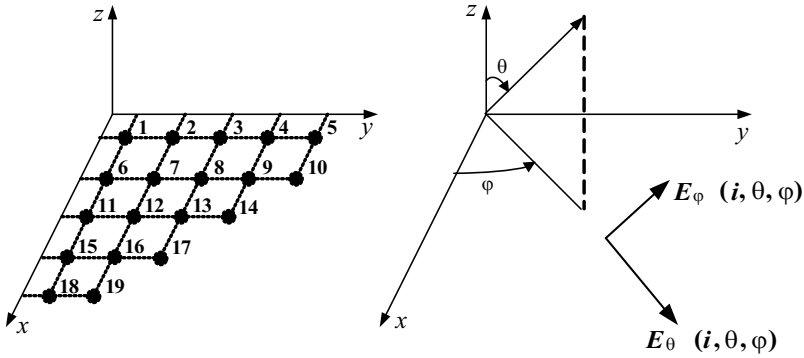

Figure 6. The coordinate system for the 19-element subarray.

where $\boldsymbol{E}_{\theta}^{m}$ $(\theta,\ \varphi)$ and $\boldsymbol{E}_{\varphi}^{m}$ $(\theta,\ \varphi)$ are the θ- and φ-components of the total vector field in the mth sideband frequency ($m = 0$ or 1, corresponding to f_0 and $f_0 + f_p$). $N = 19$ is the number of elements in the subarray. $\mathbf{E}_{\theta}(i, \theta, \varphi)$ and $\mathbf{E}_{\varphi}(i, \theta, \varphi)$ are the θ- and φ-components of the active element pattern produced by the ith element. $\boldsymbol{w}^{m}(i)$ is the equivalent excitation of the ith element, which is calculated by (2). Quantities in boldface type are vectors, and the active element patterns contain both magnitude and phase data. As the active element pattern represents the pattern radiated by the entire array when only one element is directly excited and the other elements are parasitically excited by the active element, it includes the effects of mutual coupling and the platform.

The total field pattern radiated by the fully excited array can be accurately expressed combining the two parts, $\boldsymbol{E}_{\theta}$ and $\boldsymbol{E}_{\varphi}$, given by

$$|\mathbf{E}_{total}^{m}(\theta, \varphi)| = \sqrt{\left|\mathbf{E}_{\theta}^{m}(\theta, \varphi)\right|^{2} + \left|\mathbf{E}_{\varphi}^{m}(\theta, \varphi)\right|^{2}} \tag{4}$$

In general, the co-polarization and cross-polarization patterns are paid more attention to, which can be expressed as

$$\mathbf{E}_{co\text{-}pol} = \mathbf{E}_{\theta}\cos(\varphi) - \mathbf{E}_{\varphi}\sin(\varphi), \quad \mathbf{E}_{cross\text{-}pol} = \mathbf{E}_{\theta}\sin(\varphi) + \mathbf{E}_{\varphi}\cos(\varphi) \tag{5}$$

Based on the simulation of the array in HFSS, the cross-polarization component level is -40 dB lower than the co-polarization component level, which implies that the co-polarization field pattern can be expressed approximately with the total field pattern. In the following, all the radiation patterns refer to the total field patterns.

3.3. Acquisition of Active Element Patterns

The key problem of the active element pattern method is how to acquire the active pattern data in an easy way. For the aforementioned array with 19 elements, even if the array response is computed at the azimuth planes from $\varphi = 0^{\circ}$ to 90° at a step of 10°, there are still 19×10 sets of data recording the amplitude and phase of both the $\mathbf{E}_{\theta}$ and $\mathbf{E}_{\varphi}$ components. Obviously, it is a rather cumbersome task to obtain these data after changing the port excitations in HFSS manually.

In order to solve this problem, an effective procedure has been developed to acquire the active element pattern data, as shown in Figure 7, with the help of the .vbs interface program readable by HFSS. With the procedure the 19 elements are excited individually in turn with unity terminal voltage and zero phase while the other elements are under matched load conditions. The .vbs file can be used to control the HFSS, change the port excitations and export the pattern data automatically. In order to reduce the numerical computation burden,

the complex active pattern data including $\mathbf{E}_\theta$ and $\mathbf{E}_\varphi$ are computed and recorded every 10 degrees in φ from 0° to 90° and every 2 degrees in θ from 0° to 90°. The acquisition of 190 sets of active element pattern data is finished on a PC without any manual operation. It takes only about 6 minutes to get all the data in need.

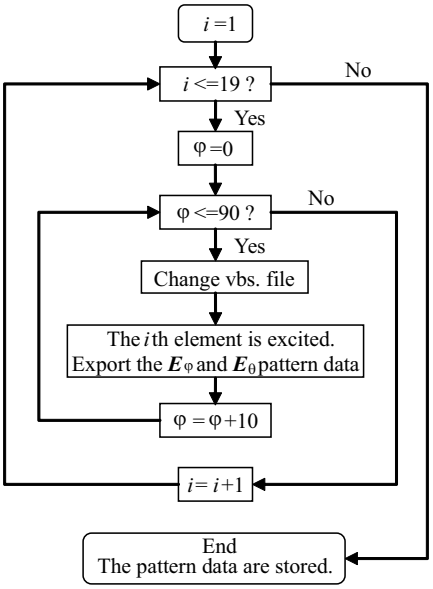

Figure 7. Flowchart of acquiring the active pattern data with the help of the vbs. interface program.

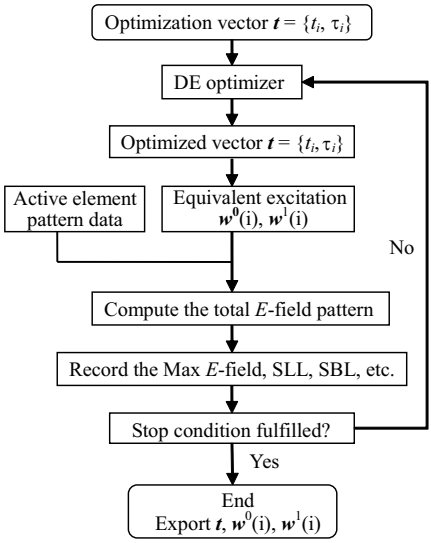

Figure 8. Flowchart of the pattern synthesis approach combining the active pattern data and the DE algorithm.

3.4. Pattern Synthesis Using the DE Algorithm

Now, the pattern synthesis procedure based on the combination of the active element pattern data and the DE algorithm is introduced, as shown in Figure 8. The DE algorithm is used to optimize the time sequences, and then the equivalent amplitude and phase excitations can be obtained by (2). According to (3) and (4), the radiation pattern of the subarray can be computed, including max E-field, SLL, SBL, which are fed back to the cost function. The DE algorithm will optimize the time sequences until the stop condition is fulfilled.

The switch-on time t_i and the on-off time interval τ_i for each element constitute the optimization parameter vector $\mathbf{t} = \{t_i, \tau_i\}$ $(i = 1, 2, \ldots, 19)$, and the cost function for a low SLL sum pattern

is constructed and given by

$$f(\mathbf{t}) = \alpha_1 \cdot \max(\mathbf{E}_{total}(\mathbf{t}))\,|_{f_0} + \alpha_2 \cdot \mathrm{SLL}(\mathbf{t})\,|_{f_0} + \alpha_3 \cdot SBL(\mathbf{t})\,\big|_{f_0+f_p} \quad (6)$$

where $\max(\mathbf{E}_{total})$ is the maximum amplitude of the total E-field at f_0, which is related to the gain of the array. SLL is the computed sidelobe level at f_0, and SBL is the computed sideband level at $f_0 + f_p$. α_1, α_2, and α_3 are corresponding weighting factors for each term.

Although the pattern synthesis approach is presented for 4D arrays, it can be slightly modified and applied to conventional arrays by ignoring the sideband radiation pattern (the term of SBL).

4. NUMERICAL RESULTS

The optimization target is to synthesize a -30 dB SLL pattern at the center frequency f_0, while suppressing the SBL to be as low as possible. The search ranges for the switch-on time t_i ($i = 1, 2, \ldots, 19$) and on-off time interval τ_i are chosen as [0, 1.0] and [0.1, 1.0], respectively.

Figure 9 shows the normalized far field patterns in different azimuth planes at f_0. Due to the additional degree of design freedom in 4D arrays, the optimized SLL can be lowered to -30.0 dB. It is known that the SLL of a conventional uniformly excited planar array without time modulation is about -16 dB. Thus, the time modulation in 4D arrays achieves a SLL reduction of about -14 dB. Figure 10 illustrates the pattern of the first sideband signal. It is seen that the SBL is suppressed to -28.5 dB. The corresponding pulse shifting time sequences are plotted in Figure 11 where the gray part means that the switches are ON.

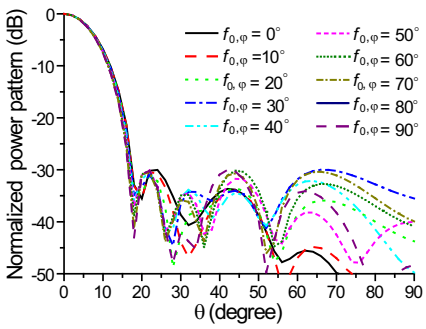

Figure 9. Computed radiation pattern at the center frequency for the 19-element subarray with time-modulation.

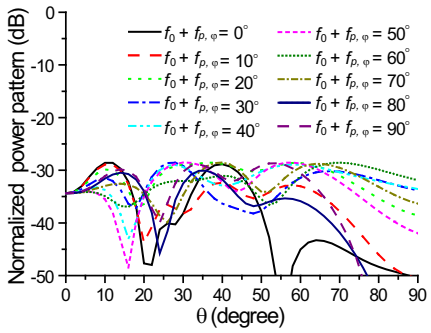

Figure 10. Computed radiation pattern at the first sideband frequency for the 19-element subarray with time-modulation.

In conventional arrays, the low SLL can be used to significantly reduce the probability of interception (LPI) in wireless communication or radar. However, a receiver sensitive enough can still eavesdrop on the information by capturing the radio waves from the sidelobes when the array is used as a transmitting antenna. In the 4D array aforementioned, the sideband signal level (shown in Figure 10) is almost as high as the center frequency signal level (shown in Figure 9) in the sidelobe region. When the proposed array is used to transmit a broadband signal, the radiated signals in the sidelobes will be time-modulated and become distorted due to aliasing effect, preventing eavesdroppers from demodulating the transmitted signal correctly. This distinct advantage in 4D arrays is useful in wireless secure communication.

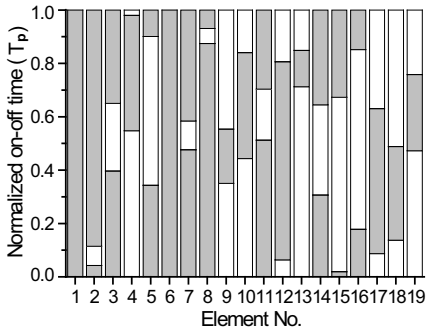

Figure 11. Optimized time sequence for the low SLL pattern in the 19-element subarray.

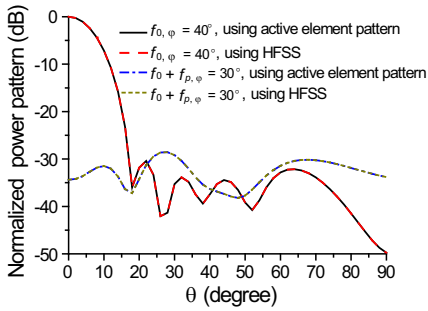

Figure 12. Comparison of the computed patterns and simulated patterns using HFSS.

To verify the proposed approach, we edited the port excitation sources of the array model in HFSS according to the equivalent excitations obtained by (2). The directly simulated results from HFSS are compared to the computed results using active element pattern data, as shown in Figure 12. It is seen that the computed results using active element pattern data are in exact agreement with the simulated results by HFSS, thus demonstrating the validity of the proposed approach.

To verify the proposed approach further, the full planar array with 76 elements is also simulated with the equivalent excitations. Figure 13 shows the simulated far field pattern at the center frequency f_0 from $\varphi = 0^\circ$ to 45°. It can be clearly seen that the SLLs in different azimuth planes are all about -30.0 dB. The front-to-back ratio of the 76-element planar array is about 38 dB. The patterns in other azimuth planes have the same results. For more intuitive view, Figure 14 illustrates the

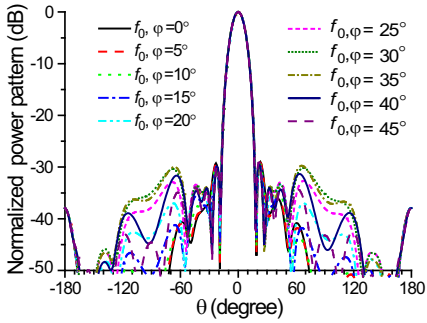

Figure 13. Simulated radiation pattern of the 76-element array in different azimuth planes.

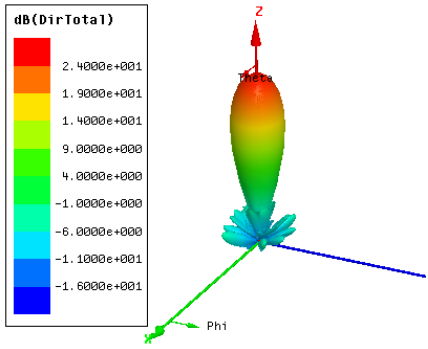

Figure 14. Simulated 3D pattern of the 76-element array with a −30 dB relative SLL.

3D radiation pattern. The simulated realized gain is 23.3 dBi for the −30 dB SLL pattern (without taking into account the feed network), while the simulated gain of the same array without time modulation is about 24.2 dBi. That is to say, the gain of the 4D array has a reduction of 0.8 dB due to the time modulation.

5. CONCLUSION

In this paper, a low sidelobe 4D planar array with 76 printed dipole elements has been designed, taking into account the effects of the mutual coupling and the surrounding environment. The commercial full-wave simulation software HFSS is used to simulate the array response. A useful interface program has been presented to obtain the large quantities of active pattern data. Based on the use of active element pattern data, a −30 dB SLL pattern is synthesized. Simulated results using HFSS verify further the effectiveness of the proposed approach. The proposed approach is commom and can be applied to arbitrary arrays of any type of elements, as long as the arrays response can be simulated by software.

ACKNOWLEDGMENT

This work was supported in part by the Natural Science Foundation of China (Grant Nos. 61125104, 61231001), the 111 project of China (Grant No. B07046) and in part by the Program for Innovation Team in University (No. IRT1113).

REFERENCES

1. Shanks, H. E. and R. W. Bickmore, "Four-dimensional electromagnetic radiators," *Can. J. Phys.*, Vol. 37, 263–275, Mar. 1959.
2. Kummer, W. H., A. T. Villeneuve, T. S. Fong, and F. G. Terrio, "Ultra-low sidelobes from time-modulated arrays," *IEEE Trans. Antennas Propag.*, Vol. 11, 633–639, Nov. 1963.
3. Yang, S., Y. B. Gan, and A. Qing, "Sideband suppression in time-modulated linear arrays by the differential evolution algorithm," *IEEE Antennas Wireless Propag. Lett.*, Vol. 1, 173–175, Dec. 2002.
4. Yang, S., Y. B. Gan, and P. K. Tan, "Comparative study of low sidelobe time modulated linear arrays with different time schemes," *Journal of Electromagnetic Waves and Application,* Vol. 18, No. 11, 1443–1458, 2004.
5. Yang, S., Y. Chen, and Z. Nie, "Simulation of time modulated linear antenna arrays using the FDTD method," *Progress In Electromagnetics Research*, Vol. 98, 175–190, 2009.
6. Pal, S., S. Das, and A. Basak, "Design of time-modulated linear arrays with a multi-objective optimization approach," *Progress In Electromagnetics Research B*, Vol. 23, 83–107, 2010.
7. Rocca, P., L. Poli, G. Oliveri, and A. Massa, "A multi-stage approach for the synthesis of sub-arrayed time modulated linear arrays," *IEEE Trans. Antennas Propag.*, Vol. 59, 3246–3254, 2011.
8. Zhu, Q., S. Yang, L. Zheng, and Z. Nie, "A pattern synthesis approach in four dimensional antenna arrays with practical element models," *Journal of Electromagnetic Waves and Applications*, Vol. 25, No. 16, 2274–2286, 2011.
9. Chen, Y., S. Yang, and Z. Nie, "Synthesis of satellite footprint patterns from time-modulated planar arrays with very low dynamic range ratios," *Int. J. Numer. Model*, Vol. 21, 493–506, 2008.
10. Poli, L., P. Rocca, L. Manica, and A. Massa, "Time modulated planar arrays analysis and optimization of the sideband radiations," *IET Microw. Antennas Propag.*, Vol. 4, No. 9, 1165–1171, 2010.
11. Rocca, P., L. Poli, G. Oliveri, and A. Massa, "Synthesis of time-modulated planar arrays with controlled harmonic radiations," *Journal of Electromagnetic Waves and Applications,* Vol. 24, Nos. 5–6, 827–838, 2010.
12. Li, G., S. Yang, Y. Chen, and Z. Nie, "A novel electronic beam steering technique in time modulated antenna arrays," *Progress*

In Electromagnetics Research, Vol. 97, 391–405, 2009.

13. Poli, L., P. Rocca, G. Oliveri, and A. Massa, "Harmonic beamforming in time-modulated linear arrays," *IEEE Trans. Antennas Propag.*, Vol. 59, 2538–2545, 2011.
14. Tennant, A., "Experimental two-element time-modulated direction finding array," *IEEE Trans. Antennas Propag.*, Vol. 58, No. 3, 986–988, Mar. 2010.
15. Hong, T., M. Song, and Y. Liu, "RF directional modulation technique using a switched antenna array for communication and direction-finding applications," *Progress In Electromagnetics Research*, Vol. 120, 195–213, 2011.
16. Rocca, P., L. Manica, L. Poli, and A. Massa, "Synthesis of compromise sum-difference arrays through time-modulation," *IET Radar Sonar Navig.*, Vol. 3, 630–637, 2009.
17. Rocca, P., L. Poli, L. Manica, and A. Massa, "Synthesis of monopulse time-modulated planar arrays with controlled sideband radiation," *IET Radar Sonar Navig.*, Vol. 6, 432–442, 2012.
18. Poli, L., P. Rocca, G. Oliveri, and A. Massa, "Adaptive nulling in time-modulated linear arrays with minimum power losses," *IET Microw. Antennas Propag.*, Vol. 5, 157–166, 2011.
19. Rocca, P., L. Poli, G. Oliveri, and A. Massa, "Adaptive nulling in time-varying scenarios through time-modulated linear arrays," *IEEE Antennas Wireless Propag. Lett.*, Vol. 11, 101–104, 2012.
20. Hong, T., M. Song, and Y. Liu, "RF directional modulation technique using a switched antenna array for physical layer secure communication applications," *Progress In Electromagnetics Research*, Vol. 116, 363–379, 2011.
21. Kelley, D. F. and W. L. Stutzman, "Array antenna pattern modeling methods that include mutual coupling effects," *IEEE Trans. Antennas Propag.*, Vol. 41, No. 12, 1625–1632, Dec. 1993.
22. Oliveri, G., L. Manica, and A. Massa, "On the impact of mutual coupling effects on the PSL performances of ADS thinned arrays," *Progress In Electromagnetics Research B*, Vol. 17, 293–308, 2009
23. Darwood, P., P. N. Fletcher, and G. S. Hilton, "Mutual coupling compensation in small planar array antennas," *IEE Proc. — Microw. Antennas Propag.,* Vol. 145, No. 1, 1–6, Feb. 1998.
24. Yuan, T., L. Li, M. Leong, J. Li, and N. Yuan, "Efficient analysis and design of finite phased arrays of printed dipoles using fast algorithm: Some case studies," *Journal of Electromagnetic Waves and Applications*, Vol. 21, No. 6, 737–754, 2007.
25. Pozar, D. M., "The active element pattern," *IEEE Trans.*

Antennas Propag., Vol. 42, No. 8, 1176–1178, Aug. 1994.

26. Yang, S. and Z. Nie, "Mutual coupling compensation in time modulated linear antenna arrays," *IEEE Trans. Antennas Propag.*, Vol. 53, No. 12, 4182–4185, Dec. 2005.
27. Bernardi, G., M. Felaco, and M. D'Urso, "A simple strategy to tackle mutual coupling and platform effects in surveillance systems," *Progress In Electromagnetics Research C*, Vol. 20, 1–15, 2011.
28. He, Q. and B. Wang, "Design of microstrip array antenna by using active element pattern technique combining with Taylor synthesis method," *Progress In Electromagnetics Research*, Vol. 80, 63–76, 2008.
29. He, Q., B. Wang, and W. Shao, "Radiation pattern calculation for arbitrary conformal arrays that include mutual-coupling effects," *IEEE Antennas Propag. Magazine*, Vol. 52, No. 2, 57–63, Apr. 2010.
30. Pozar, D. M., "A relation between the active input impedance and the active element pattern of a phased array," *IEEE Trans. Antennas Propag.*, Vol. 51, No. 9, 2486–2489, Sep. 2003.
31. Kelley, D. F., "Relationships between active element patterns and mutual impedance matrices in phased array antennas," *Proc. IEEE Antennas Propag. Symp.*, 524–527, 2002.
32. Pal, S., B.-Y. Qu, S. Das, and P. N. Suganthan, "Optimal synthesis of linear antenna arrays with multi-objective differential evolution," *Progress In Electromagnetics Research B*, Vol. 21, 87–111, 2010.
33. Li, R., L. Xu, X.-W. Shi, N. Zhang, and Z.-Q. Lv, "Improved differential evolution strategy for antenna array pattern synthesis problems," *Progress In Electromagnetics Research*, Vol. 113, 429–441, 2011.
34. Rocca, P., G. Oliveri, and A. Massa, "Differential evolution as applied to electromagnetics," *IEEE Antennas Propag. Magazine*, Vol. 53, 38–49, 2011.
35. Zhu, X., S. Yang, and Z. Nie, "Full-wave simulation of time modulated linear antenna arrays in frequency domain," *IEEE Trans. Antennas Propag.*, Vol. 56, No. 5, 1479–1482, 2008.
36. Poli, L., P. Rocca, L. Manica, and A. Massa, "Pattern synthesis in time-modulated linear arrays through pulse shifting," *IET Microw. Antennas Propag.*, Vol. 4, No. 9, 1157–1164, 2010.